Postdoc Fellowships for non-EU researchers

Final Report

Name	Rahul Kumar
Selection	BELSPO 2013
Host institution	Dept. of Plant System Biology/VIB, Ghent University
Supervisor	Prof. Dr. Eugenia Russinova
Period covered by this report	from 27/08/2014 to 24/02/2016
Title	Probing the molecular mechanisms underlying AP2-mediated internalization of brassinosteroid receptor complex in *Arabidopsis*

1. Objectives of the Fellowship (1/2 page)

Brassinosteroids (BRs) play diverse roles in plant growth and development, including vegetative and reproductive development, germination, senescence, and responses to various biotic and abiotic stresses. The perception of BRs at the plasma membrane (PM) by their receptor BR INSENSITIVE1 (BRI1) and consequent downstream signaling pathway have been studied in detail during the past decade (Wang et al., 2012). Briefly, BR dependent auto- and trans-phosphorylation of BRI1 and BAK1 participate in receptor complex activation, modulate a cellular cascade of kinases and phosphatases and activates two downstream transcription factors, BRASSINAZOLE-RESISTANT1 (BZR1) and BRI1-EMS SUPPRESSOR1 (BES1). These transcription factors bind to the target promoters in the presence of different interacting partners to regulate BR genomic responses. During BR signaling, BRI1 constitutively cycles between the PM and the *trans*-Golgi network/early endosome (TGN/EE). Successful implication of a bioactive, fluorescent BR analog, Alexa Fluor 647–castasterone (AFCS), tool to visualize the endocytosis of BRI1-AFCS complexes in living *Arabidopsis thaliana* cells has established that the majority of BR signaling is initiated by the PM pool of BRI1 (Irani et al., 2012). The ADAPTOR PROTEIN COMPLEX-2 (AP-2), which assists the formation of clathrin-coated vesicles at the PM is also essential for BRI1 endocytosis. The knockdown of AP2A1, one of the AP-2 subunits, results in impaired BRI1 endocytosis and enhanced the brassinosteroid signaling in *Arabidopsis* (Rubbo et al., 2013). However, the motifs responsible for this interaction between BRI1 and AP-2 remain unknown. In mammalian systems, interaction between AP-2 complex and the cargo proteins depends on the presence of three motifs in the cargos: YXXΦ, [D/E]XXXL[L/I] and FXNPXY (Bonifacino and Traub, 2003; Traub, 2009). The Tyr-to-Ala substitutions in YXXΦ has been found to interfere with endocytosis of the tomato receptor EIX2 and BOR1 (Bar and Avni, 2009; Takano et al., 2010). In addition, AP2M binds to VSR-PS1 via a YXXΦ motif in vitro (Happel et al., 2004). These evidences suggest that a similar cargo recognition mechanism by AP2-complex would operate during early events of BRI1 endocytosis. Although, several putative YXXΦ motifs are present in its intracellular kinase domain (Geldner and Robatzek, 2008), BRI1 protein is devoid of canonical [D/E]XXXL[L/I] motifs. We speculated two possibilities for AP-2-mediated endocytosis of BRI1. First possibility is that AP-2 recognizes noncanonical motifs in the cargo proteins, of which the sequences have not yet been identified. The second possible scenario is that an unknown internalization motif-carrying factor (a BRI1 coreceptor or another BRI1-interacting protein) is recognized by AP-2 and, in turn, bridges the interaction with BRI1. Therefore, aims of the present work are:

I. To elucidate the mechanisms underlying BRI1 recognition by AP-2 complex by mutant analysis of both putative YXXΦ and identified atypical XLL motifs present in BRI1 kinase domain.

II. To identify BRI1-interacting partners, which might not directly involved BR signaling but would help understand the BRI recognition and its subsequent internalization, using a proteomics approach. Overall, results from this study will provide clues for how BRI is recognized at PM and internalized and how AP-2 complex is important for this whole process.

2. Methodology in a nutshell (1/2/ page)

In order to achieve the objectives, both advanced and state-of-art computational, molecular and cell biology and Confocal Laser Scanning Microscopy (CLSM) techniques were used.

1. The conserved YXXΦ and XLL motifs in the cytoplasmic region of BRI1 protein were predicted by homology search. The identified domains were checked for their surface exposed nature by superimposing the protein sequence on the already available crystallized BRI1 kinase domain 3-D structure.
2. The BRI1 mutant alleles for XLL and the surface exposed and YXXΦ motifs were generated using Site-Directed Mutagenesis.
3. Transgenic plants for the mutated BRI1 alleles along with their control (BRI1-complemeted line) were generated by introducing these alleles in *bri1-116* and *bri1-GABI-Kat* mutant background, respectively.
4. The homozygous nature of transgenic lines for transgene insertion and mutant background were confirmed by using growing the seeds on ½ MS medium complemented with the respective antibiotics and genotyping for *BRI1* gene, respectively.
5. Transcript and protein levels of BRI1 in Col-0 and different transgenic lines were determined by employing quantitative real time PCR (qPCR) and western blot analysis for *BRI1* gene.
6. Complementation of *bri1-116* and /or *bri1-GABI-Kat* mutant inhibited growth phenotypes were studied in the normal and mutated BRI1 transgenic lines by growing seeds on ½ MS. The altered BR signaling in these mutants was observed by studying their hyper/hypo sensitive nature against the brassinolide (BL) and brassinazole (BRZ). For this analysis, seeds were placed on ½ MS supplemented with BL or BRZ and grown in both light and dark and root and hypocotyl length measurement was performed after 5 days. In addition, rosette leaf are analysis of Col-0, BRI1-complemeted and mutated BRI1 transgenic lines were performed by growing seeds on ½ MS for 15-days.
7. The BR signaling in the Col-0, BRI1-complemeted and mutated BRI1 transgenic lines under both normal and BL-activated growth conditions were studied by measuring the dephosphorylation of BES1 protein using anti-BES1 antibody in western blot analysis.
8. Spinning disc confocal microscopy was employed to compare the BRI1 retention time on PM between BRI1-complemeted and mutated BRI1 transgenic lines. Microscopy was performed in the hypocotyls of 5-day-old dark grown seedlings. Imaging speed was set at 1 image/sec and total imaging time as kept 180 seconds. Finally, the BRI1 retention time on PM was determined by track length analysis on kymographs using ImageJ.
9. BRI1 interactome was identified by employing Mass spectrometry-based immunoprecipitation (IP) proteomics approach. For this purpose, BRI1-GFP transgenic lines (in Col-0 and *gnl1* mutant backgrounds) were used. IP was carried out using anti-GFP antibody. The IPed samples were digested by trypsin and purified using a custom made columns. The purified samples were used for detection of co purified proteins with BRI1 using GC-MS. The Col-0 samples processed at the same time were used for normalization of the BRI1-GFP transgenic lines.

3. Results (6-8 pages)

Six YXXΦ and three atypical XLL motifs are present in BRI1 kinase domain

Based on the recently updated crystal structures of phosphorylated BRI1 kinase domain (Bojar et al., 2014), we identified six surface exposed putative YXXΦ motifs at 898, 945, 956, 961, 1058 and 1072 aa in the kinase domain of BRI1 (Figure 1). These motifs are projected outwards, making them amenable for assisting interactions with cargo protein. Similarly, three putative XLL motifs at 875, 950 and 1124 aa in its kinase domain and one conserved but with an unknown function FSTI motif at 1177 aa was identified at the C-terminal of BRI1.

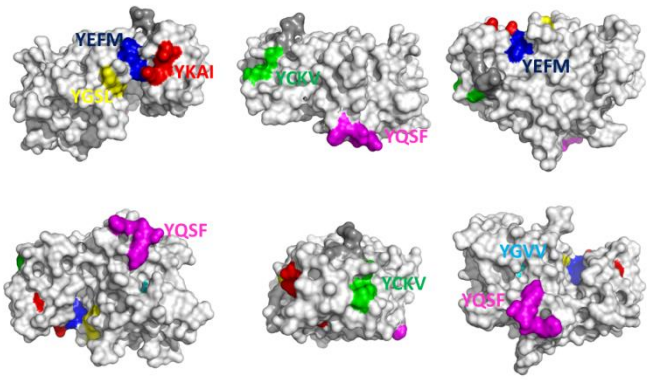

Figure 1. Schematic representation of the predicted YXXΦ motifs in BRI1 kinase domain. The respective positions of these domains in the kinase domain as follow: YKAI-898; YCKV-945; YEFM-956; YGSL-961; YQSF-1058; YGVV-1072. The predicted domains are projected outward and exposed to protein surface. Each motif is depicted by a different color.

Generation of XLL and YXXΦ mutant transgenic lines in *Arabidopsis*

In order to characterize their role, stable pBRI1::BRI1-GFP/*bri1-116* and pBRI1::BRI1-mCitrine/*bri1-GABI-Kat* transgenic lines for mutated XLL and YXXΦ motifs, respectively, were generated in *Arabidopsis*. The details of mutations in the putative XLL motifs (M1-M3) are presented in Figure 2. The homology search of *Arabidopsis* BRI1-cytoplasmic domain with its homologs led to identification of a conserved motif (M4) at its carboxy end. To elucidate its putative function in BR signaling, we also obtained transgenic lines for its normal and mutated alleles. In case of YXXΦ motifs substitution transgenic lines, tyrosine (Y) aa was changed by phenylalanine (F) to keep the similar structure.

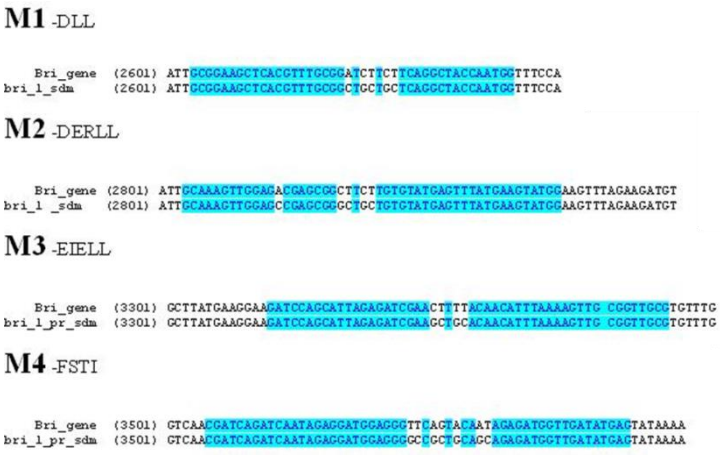

Figure 2. Details of the base substitutions in the putative XLL motifs, used in the generation of stable transgenic pBRI1:BRI1(M)-GFP/*bri1-116* lines in *Arabidopsis*. (M) depicts the mutations in different XLL motifs. In addition, pBRI1:BRI1-GFP/*bri1-116* transgenic lines were also generated.

Additionally, tyrosine to serine (Y to S) mutations were created for motifs present at 898 and 956 aa. These mutants were created to keep these sites amenable for phosphorylation and thus to maintain the kinase activity of mutated BRI1 alleles. The details of different Y to F and Y to S mutations of YXXΦ motif is given in Table 1.

TyrxxØ mutant Constructs	Transformed genotype
pK7m34GW-pBRI1::BRI1-Y831F-mCitrine	Heterozygous bri1-Gabi Arabidopsis plants
pK7m34GW-pBRI1::BRI1-Y898F-mCitrine	Heterozygous bri1-Gabi Arabidopsis plants
pK7m34GW-pBRI1::BRI1-Y945F-mCitrine	Heterozygous bri1-Gabi Arabidopsis plants
pK7m34GW-pBRI1::BRI1-Y956F-mCitrine	Heterozygous bri1-Gabi Arabidopsis plants
pK7m34GW-pBRI1::BRI1-Y961F-mCitrine	Heterozygous bri1-Gabi Arabidopsis plants
pK7m34GW-pBRI1::BRI1-Y1058F-mCitrine	Heterozygous bri1-Gabi Arabidopsis plants
pB7m34GW-pBRI1::BRI1-Y898S-mCitrine	Heterozygous bri1-Gabi Arabidopsis plants
pB7m34GW-pBRI1::BRI1-Y956S-mCitrine	Heterozygous bri1-Gabi Arabidopsis plants
pB7m34GW-pBRI1::BRI1-Y1058S-mCitrine	Heterozygous bri1-Gabi Arabidopsis plants
pK7m34GW-pBRI1::BRI1-mCitrine	Heterozygous bri1-Gabi Arabidopsis plants

Table 1. Details of the mutations created in six YXXΦ motifs, used in the generation of stable transgenic pBRI1:BRI1(Y to F/Y to S)-mCitrine-/*bri1-GABI-Kat* lines in *Arabidopsis*.

BR signaling appears to be unaffected when the atypical XLL motifs in BRI1 were mutated

In order to study the effect of putative XLL mutations on BR signaling, we first did initial characterization of pBRI1::BRI1(M)-GFP/bri1-116 homozygous XLL mutant transgenic lines in T_4 generation. Wild type (Col-0), pBRI1::BRI1-GFP/*bri1-116* complemented line and pBRI1::BRI1(M)-GFP/*bri1-116* XLL mutant transgenic plants were grown in dark on agar plates either in the absence or presence of BRZ (500 nM), the BR biosynthetic inhibitor or BL. Hypocotyl and root length of 5-day-old seedlings grown in dark and light, respectively, were measured. For quantitative real time PCR analysis of *BRI1* in these lines, 5-day old light grown seedlings were used. The expression profiling of *BRI1* in Col-0, pBRI1::BRI1-GFP/*bri1-116* and these transgenic lines showed that pBRI1::BRI1(M2)-GFP-1.2 (presented as M2GFP-1.2) and pBRI1::BRI1(M4)-GFP-2.7 (presented as M4GFP-2.7) were the overexpression lines whereas the remaining mutant transgenic lines accumulated *BRI1* transcripts at similar level as observed in Col-0 and pBRI1::BRI1-GFP/*bri1-116* complemented line (3A). We did not notice any significant difference in hypocotyl and root length between wild type, pBRI1::BRI1-GFP/*bri1-116* complemented line and most of pBRI1::BRI1(M)-GFP/*bri1-116* XLL mutant transgenic lines under tested growth conditions (Figure 3B and C). However, slightly longer hypocotyl were observed for pBRI1::BRI1(M4)-GFP-2.7/*bri1-116* (M4GFP-2.7) lines under BRZ treatment which could be due to higher transcript levels of *BRI1* in this transgenic line (Figure 3B). Nonetheless, no such change in root length of this transgenic line under BL-activated condition was observed (Figure 3C).

BR signaling is reduced in BRI1 (Y to S) mutant transgenic lines

qPCR and western blot analyses were employed to determine the BRI1 transcript and protein levels, respectively, in Col-0, pBRI1::BRI1-mCitrine complemented line and BRI1(Y to S) mutant transgenic lines (Figure 4A and B). Similar analyses between Col-0, pBRI1::BRI1-mCitrine/*bri1-GABI-Kat* complemented line, pBRI1::BRI1(Y898S)-mCitrine/*bri1-GABI-Kat* (presented as Y898S in figure) and pBRI1::BRI1(Y956S)-mCitrine/*bri1-GABI-Kat* (presented as Y956S in figure) lines revealed

(homozygous T_4 generation) that seedlings of pBRI1::BRI1(Y898S)-mCitrine/*bri1- GABI-Kat* were more sensitive to BRZ than their control (Figure 5A and B).

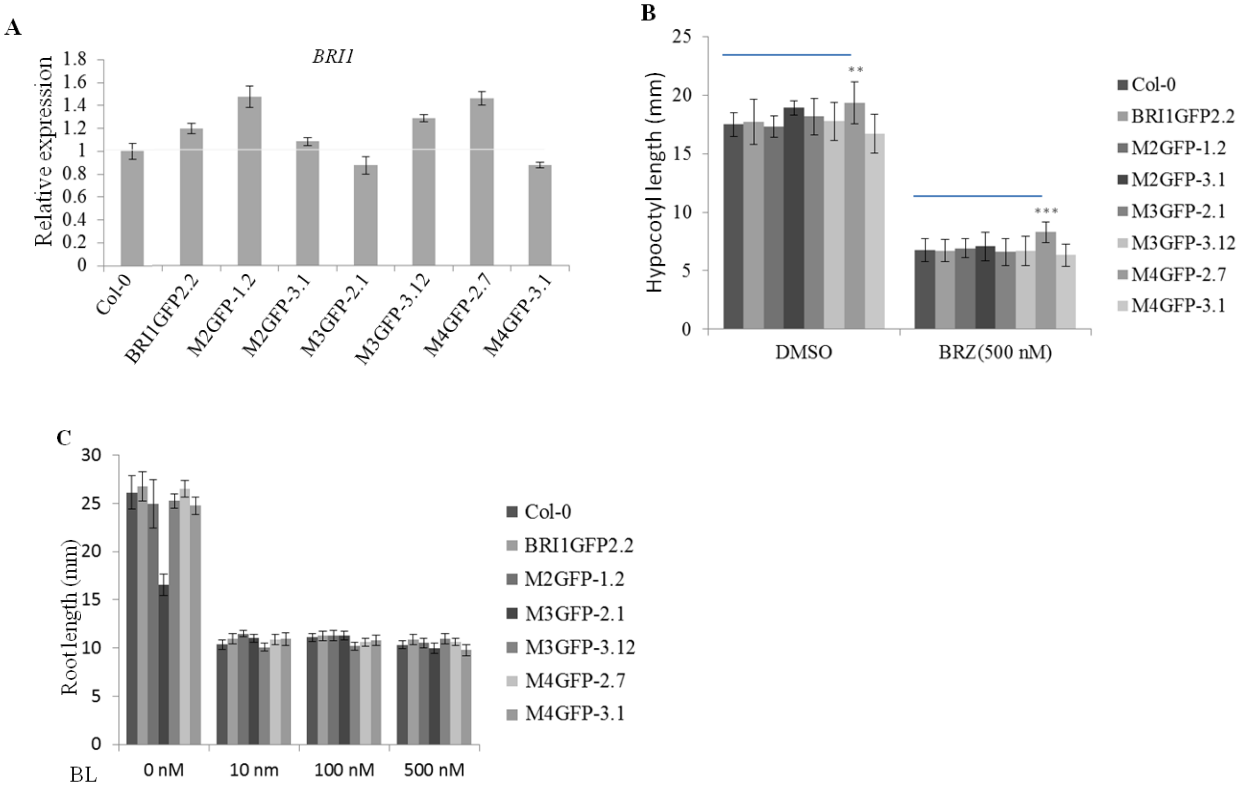

Figure 3. pBRI1::BRI1(M)-GFP/*bri1-116* XLL mutant transgenic lines do not exhibit an altered phenotype. (A) Expression profiling of *BRI1* in Col-0, pBRI1::BRI1-GFP/*bri1-116* complemented line (BRI1GFP2.2) and different XLL mutant transgenic lines. (B) Comparison of hypocotyl length of 5-day-old dark grown Col-0 (n = 30), pBRI1::BRI1-GFP/*bri1-116* complemented line (BRI1GFP2.2) and XLL transgenic line (n = 30) seedlings in the absence and presence of brassinazole (500 nM). The experiment was repeated twice. (C) Comparison of root length of 5-day-old dark grown Col-0 (n = 30), pBRI1::BRI1-GFP/*bri1-116* complemented line (BRI1GFP2.2) and XLL transgenic line (n = 30) seedlings in the absence and at different concentrations (10 nM, 100 nM and 500 nM) of BL. The experiment was repeated twice. M2, M3 and M4 represent BRI1(M2), BRI1(M3) and BRI1(M4). Statistics was done using Student's *t*-test. ** = P value >0.001 to < 0.05; *** = P value <0.001

The BRI1 (Y to S) mutant transgenic lines were found to be BL-resistant as they exhibited longer hypocotyls and roots in comparison to their controls, including Col-0 and pBRI1::BRI1-mCitrine/*bri1-GABI-Kat* complemented line under BL-activated condition (Figure 6A and B). Further, these mutant lines exhibited smaller rosette leaf area than their controls (Fig. 7A and B). Additionally, these BRI1(Y to S) mutant lines also exhibited partial male sterility as we obtained reduced seeds for them in comparison to the wild type and pBRI1::BRI1mCitrine/*bri1-GABI-Kat* lines.

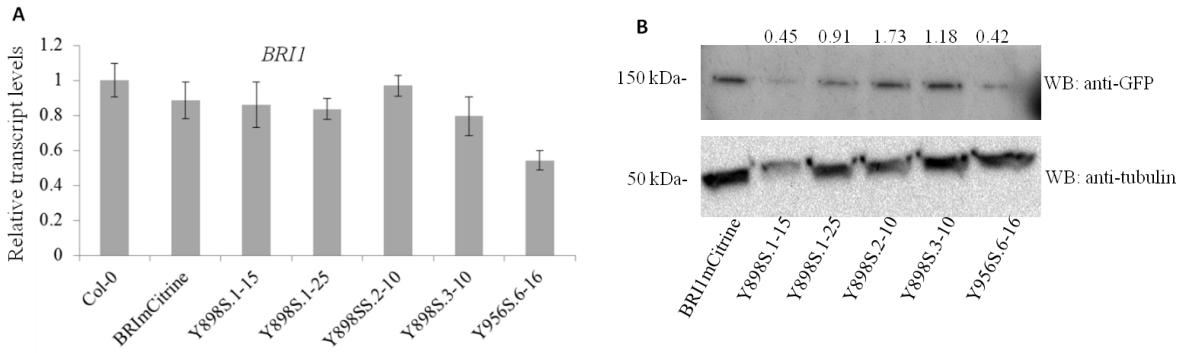

Figure 4 Expression analysis of *BRI1* in Col-0, pBRI1::BRI1mCitrine/*bri1-GABI-Kat* complemented line (BRI1mCitrine) and different BRI1 (Y to S) mutant transgenic lines by employing (A) qPCR method and (B) by determination of BRI1 protein by Western blot analysis using anti-GFP antibody. Western blot analysis using anti-α-tubulin antibody was used as a control. The number on the top of figure indicate the relative BRI1 protein level in the BRI1(Y to S) mutant transgenic lines in comparison to the their control pBRI1::BRI1-mCitrine/*bri1-GABI-Kat* complemented line.

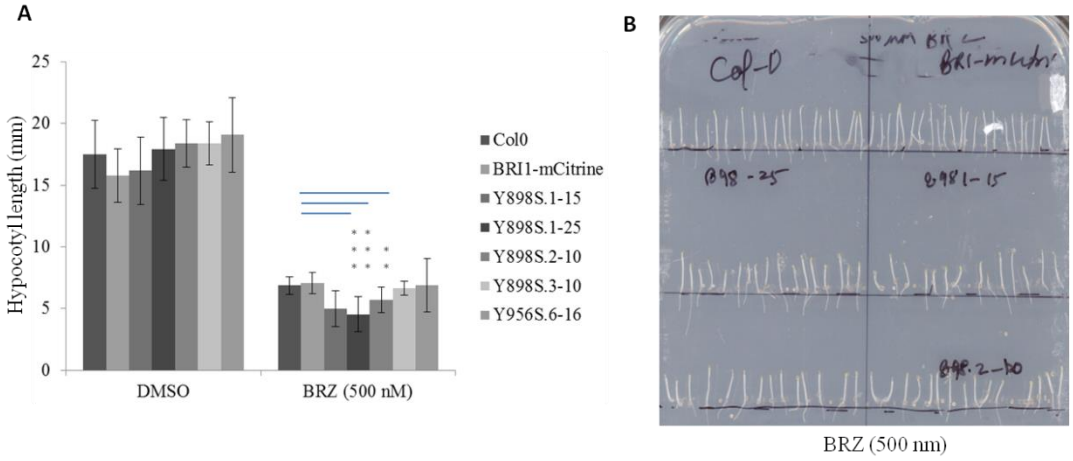

Figure 5. (A) Comparison of hypocotyl length of 5-day-old dark grown Col-0, pBRI1::BRI1-mCitrine/*bri1-GABI-Kat* complemented line (BRI1mCitrine) and BRI1 (Y to S) mutant transgenic seedlings in the absence and presence of BRZ (500 nM). The experiment was repeated twice. Y898S and Y956S represent Y to S substitution at 898 and 956 aa position in BRI1 protein. (B) Representative image of the seedlings grown in dark for 5 days for the measurement of hypocotyl length under BRZ treated condition. Statistics was done using Student's *t*-test. ** = P value >0.001 to < 0.05; *** = P value <0.001. (n = 30)

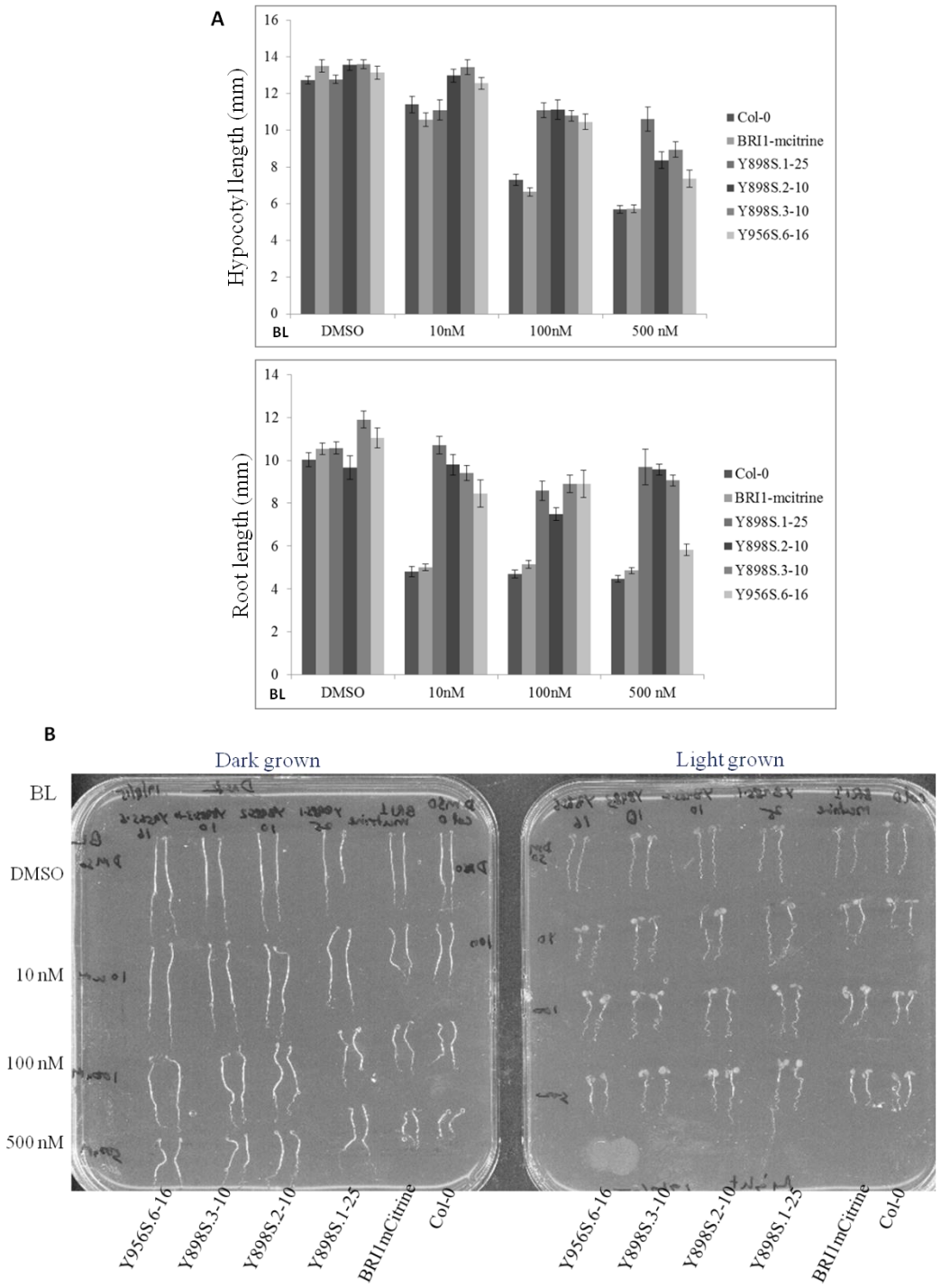

Figure 6. (A) Comparison of hypocotyl and root length of 5-day-old dark and light grown, respectively, Col-0, pBRI1::BRI1-mCitrine/*bri1-GABI-Kat* complemented line (BRI1mCitrine) and BRI1 (Y to S) mutant transgenic seedlings in BL-activated condition. The experiment was repeated twice. Y898S and Y956S represent Y to S substitution at the 898 and 956 aa position in BRI1 protein. (B) Representative image of the seedlings grown in dark for hypocotyl length and in light for root length for 5 days on 1/2 MS-agar supplemented with either DMSO or different concentrations of BL (10, 100 and 500 nM). (n = 30)

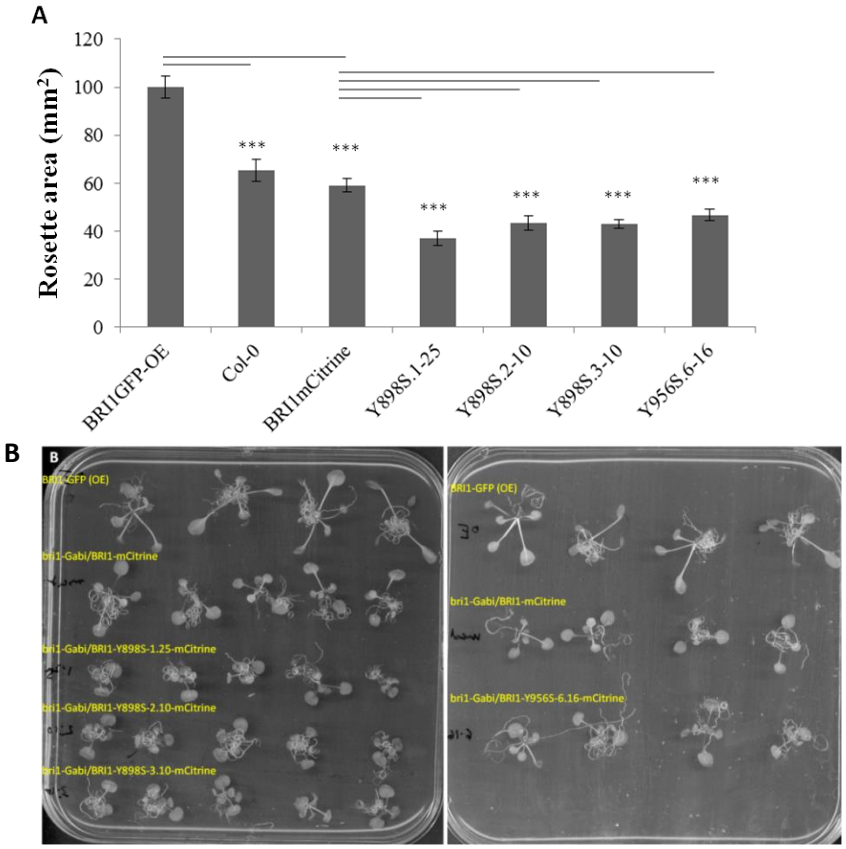

Figure 7. Rosette leaf area is reduced in BRI1 (Y to S) mutant lines (A) Comparison of rosette leaf area of two-week-old light grown Col-0, pBRI1::BRI1-mCitrine complemented line (BRI1mCitrine) and BRI1(Y to S) mutant transgenic lines. The experiment was repeated twice. (B) Representative image of the two-week-old light grown seedlings which were used in the measurement of rosette leaf area (n>40). Statistics was done using Student's *t*-test. ** = P value *** = P value <0.001.

The distinct phenotypic response shown by BRI1(Y to S) mutant lines, than their control, under both BRZ- and BL-treated conditions suggested that BR signaling might be altered in these transgenic lines. Study of dephosphorylation of BES1, a regulator of BR signaling, by western blot analysis remains a well explored read-out to determine BR signaling. Therefore, we next studied the BES1 dephosphorylation status under BL-activated conditions. It was observed that whereas most of phosphorylated BES1 was converted into its dephosphorylated form in Col-0, pBRI1::BRI1-mCitrine/*bri1-GABI-Kat* complemented line and pBRI1::BRI1-GFP overexpression lines, such conversion was found to be reduced in the BRI1(Y to S) mutant lines, suggesting inhibited BR signaling in these transgenic lines under BL-activated condition (Figure 8 A and B). We hypothesized that the inhibited BR signaling can be due to two reasons either; first, reduced kinase activity of mutant alleles or second, altered internalization of BRI1 from PM to cytoplasm. In order to validate either of the reasons, the normal as well as mutated BRI1 alleles have been processed for studying their *in vitro* kinase activity. In addition, pBRI1::BRI1-mCitrine/*bri1-GABI-Kat* and pBRI1::BRI1(Y898S)-mCitrine/*bri1-GABI-Kat* lines were used for CLSM imaging to analyze the BRI1 internalization.

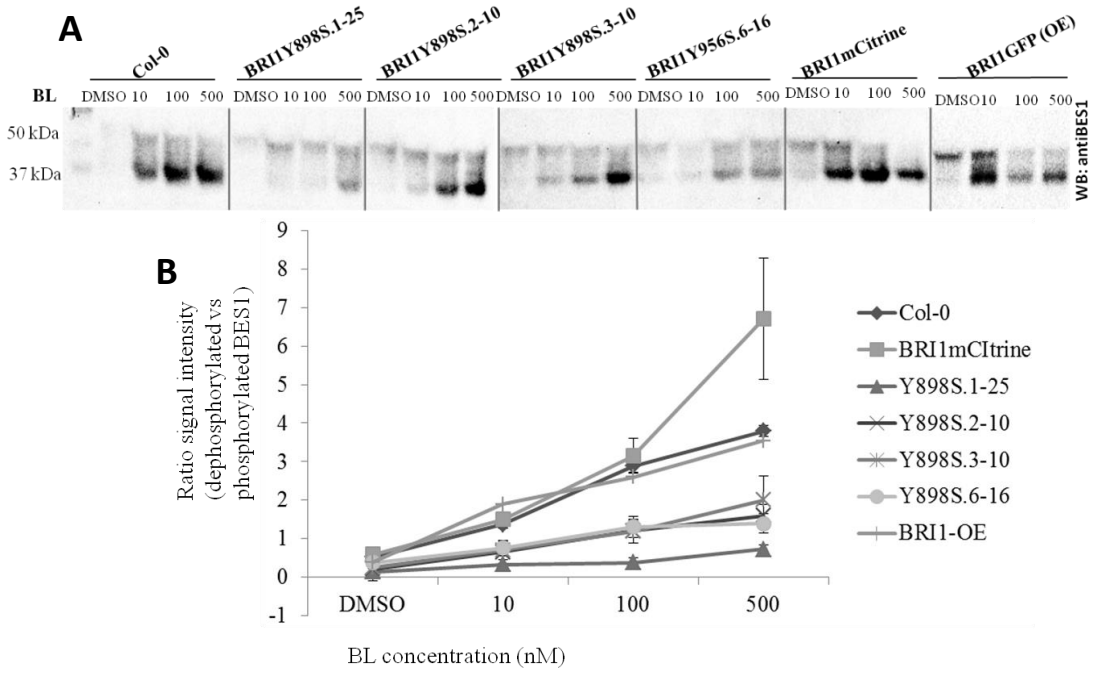

Figure 8. Reduced dephosphorylation of BES1 suggests BR signaling is inhibited in the BRI1 (Y to S) mutant transgenic lines under BL-activated growth condition. (A) Western blot analysis of BES1 activity in Col-0, pBRI1::BRI1-mCitrine complementing the *bri1-GABI-Kat* mutant (BRI1mCitrine), BRI1-GFP (BRI1-OE) and BRI1(Y to S) mutant transgenic lines under BL-activated condition. Blot was probed with the anti-BES1 antibody. The experiment was repeated three times. (B) Quantification of the ratio between dephosphorylated vs phosphorylated BES1. As shown in the graph, more BES1 was found in its dephosphorylated form in Col-0, BRI1mCitrine and BRI1-OE than BRI1 (Y to S) mutant lines.

Spinning disc imaging of pBRI1::BRI1-mCitrine/*bri1-GABI-Kat* complemented line and pBRI1::BRI1(Y898S)-mCitrine/*bri1-GABI-Kat* lines reveal that most of BRI1 at the PM remains in steady state and only a small portion is dynamic in nature

In order to determine whether BRI1 internalization is altered in the BRI1(Y to S) mutant lines, we next employed Spinning disc imaging on hypocotyls of 5-day-old etiolated seedlings to find out the retention time of BRI1 at the PM in pBRI1::BRI1m-Citrine/*bri1-GABI-Kat* (complemented line) and pBRI1::BRI1(Y898S)-mCitrine/*bri1-GABI-Kat.* The study revealed that most of the BRI1 at the PM remains in steady state and did not undergo internalization and only a small fraction of BRI1 was found to be dynamically internalized into cytoplasm in both BRI1-mCitrine/*bri1-GABI-Kat* and BRI1(Y898S)/*bri1-GABI-Kat* line (Figure 9A and B). However, interestingly, track length analysis of kymographs revealed that the BRI1 retention time was significantly prolonged in the latter (Figure 9B). Whereas over 65% of BRI1 spots showed a time of residency less than 20 seconds in BRI1m-Citrine/*bri1-GABI-Kat* line, contrastingly, over 55% spots were found to have more than 20 second of tome of residency in BRI1(Y898S)/*bri1-GABI-Kat* line (Figure 9C). Overall, an average time of BRI1 residency at PM was found to be 28 seconds in BRI1(Y898S)/*bri1-GABI-Kat* line in comparison to the 16 seconds observed in the BRI1m-Citrine/*bri1-GABI-Kat* line (Figure 9D).

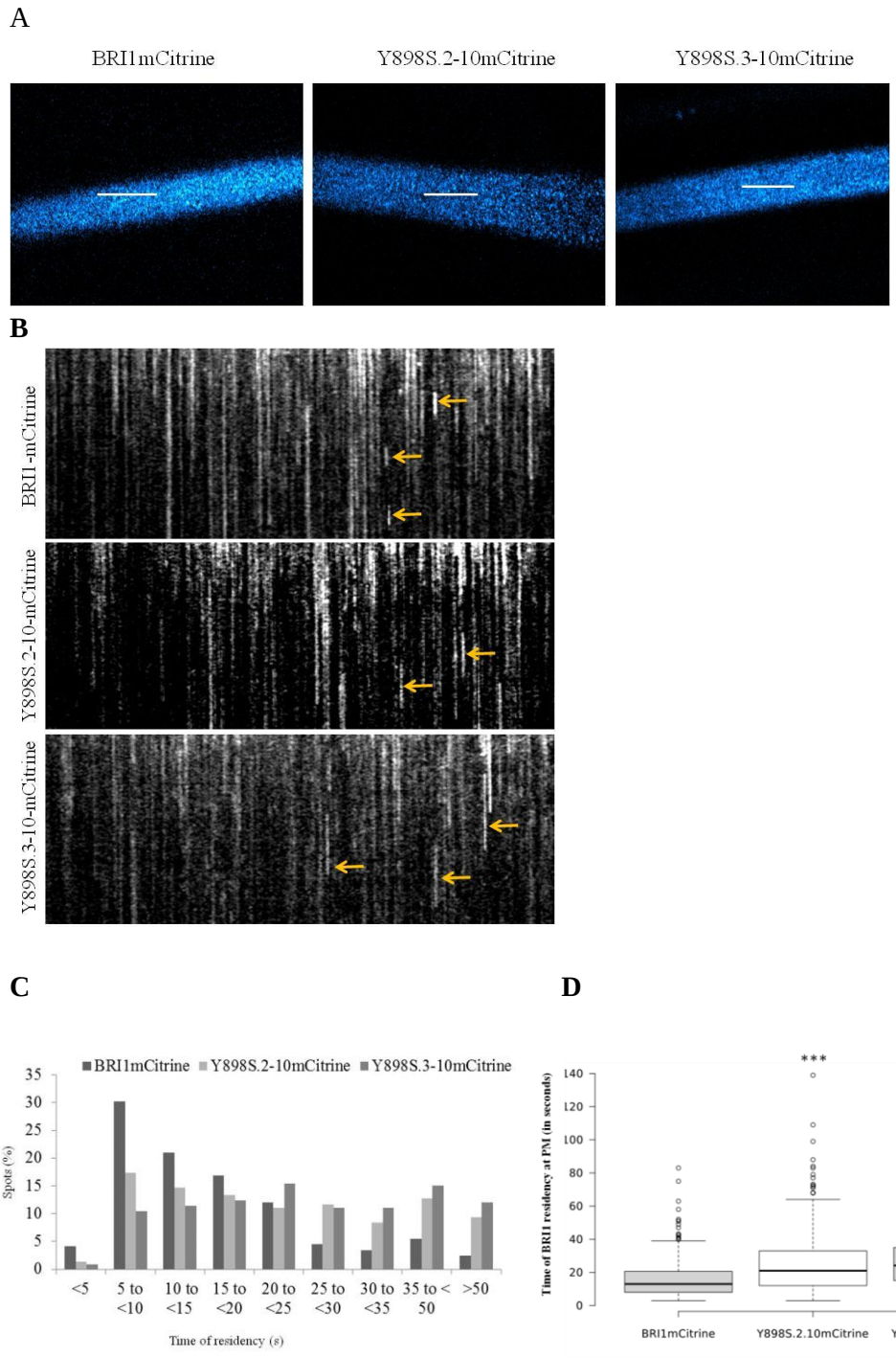

Figure 9. Spinning disc confocal microscopy of BRI1-mCitrine/*bri1-GABI-Kat* and BRI1(Y898S)/*bri1-GABI-Kat* lines suggests a longer time of residency of BRI1 in the latter. (A) Representative images of spinning disc confocal movies of BRI1m-Citrine, BRI1Y898S-2.10-mCitrine and BRI1Y898S-3.10-mCitrine (B) Representative images of kymographs with spots used for track length analysis to determine time of residency for BRI1 at plasma membrane. (C) Distribution of spots in time scale. The distribution was obtained from kymograph-based track length analyses (n>600). (D) Box plot summary of time of residency of BRI1 in BRI1-mCitrine/*bri1-GABI-Kat* and BRI1(Y898S)/*bri1-GABI-Kat* lines. Statistics was done using Student's *t*-test. *** = P value <0.001.

BR1 co-IPed with PM-localized ATPase, aquaporin, PIN3 and several receptor kinase proteins

Besides generating the YXXΦ and XLL mutant transgenic lines, we also studied the BRI1 interactome by using pBR11::BRI1-GFP transgenic plants (Geldner et al., 2007; Fàbregas et al., 2013). This transgenic line is known to accumulate BRI1 similar to endogenous levels. Both BRI1 endocytosis and BR signaling is also dependent on functional ARF-GEF proteins. In addition, effect of the unavailability of functional ARF-GEF proteins on the BRI1 interactome was studied by using pBR11::BRI1-GFP/*gnl1* genotype in absence and presence brefeldin A (BFA) drug, an inhibitor of BFA-sensitive ARF-GEFs (Peyroche et al., 1999). We studied BRI1-interactome in pBR11::BRI1-GFP transgenic plants under both normal and BL-activated condition. Additionally, this study was performed using both total protein extract as well as only microsomal fraction. This study identified several membrane localized protein such as ATPases, aquaporins, receptor like kinases such as FERONIA and Probable inactive receptor kinase, Auxin efflux carrier component 3 (PIN3), Clathrin heavy chain 2, ABC transporter G family member 36 as putative interactors of BRI1 (Table 2). However, the absence of functional ARF-GEF proteins did not found to affect this interaction as no significant change in the BRI1 interacting proteins was observed in pBR11::BRI1GFP/*gnl1* and pBR11::BRI1-GFP/*gnl1*+BFA conditions (Table 3).

TAIR ID	BRI-GFP (endo) total protein fraction	BRI-GFP (endo) Microsomal fraction 1	BRI-GFP (endo) Microsomal fraction 2	BRI-GFP (endo) Microsomal + BL
AT1G70940	✔	✔	✔	✔
AT2G18960	✔	✔	✔	✔
AT3G57330	✔	✔	✔	✔
AT1G30360	✔	✔	✔	✔
AT4G30190	✔	✔	✔	✔
ATCG00680		✔	✔	✔
AT1G06950		✔		✔
AT1G15210		✔	✔	✔
AT1G56070		✔	✔	
AT1G70410		✔	✔	✔
AT1G70770		✔	✔	✔
AT2G30520		✔	✔	✔
AT3G08530		✔		✔
AT3G08940		✔	✔	✔
At3g23750		✔	✔	✔
AT3G47730		✔	✔	✔
AT3G51550		✔	✔	✔
AT4G17530		✔		✔
At5g16590		✔	✔	✔

Table 2: Details of the BRI1 interacting proteins identified in IP-MS experiment. Five-day-old light grown *Arabidopsis* seedlings of pBR11::BRI1-GFP {with or without BL (100 nM) treatment, 2h} were used for the protein extraction (either total or only microsomal fraction) and immunoprecipitation. Table shows comparative compilation of a set of common proteins identified in most of IP/MS experiments. ✔ indicates the presence of that protein in the list.

TAIR ID	gnl1/BRI-GFP (endo) total protein fraction	gnl1/BRI-GFP (endo) Microsomal fraction 1	gnl1/BRI-GFP (endo) + BFA total protein fraction	gnl1/BRI-GFP (endo) + BFA microsomal protein fraction
AT2G18960	✔		✔	✔
AT4G30190	✔	✔	✔	✔
AT1G70940	✔	✔	✔	✔
AT3G57330	✔	✔	✔	✔
AT3G47730	✔	✔	✔	✔
AT3G08530	✔			✔
At3g14840		✔		✔
AT3G51550		✔		✔
At4g35230		✔		✔
AT4G09000		✔	✔	✔

Table 3: Details of the BRI1 interacting proteins identified in IP-MS experiment. Five-day-old light grown *Arabidopsis* seedlings of pBR11::BRI1-GFP/*gnl1* {with or without BRZ (50 µM) treatment, 2h} were used for the protein extraction (either total or only microsomal fraction) and immunoprecipitation. Table shows comparative compilation of a set of common proteins identified in most of IP/MS experiments. ✔ indicates the presence of that protein in the list.

4. Perspectives for future collaboration between units

We have aimed to gain mechanistic understanding of the molecular mechanisms underlying AP-2 complex-mediated internalization of BRI1 in *Arabidopsis*. The recognition by AP2-complex is an important step in the internalization of membrane localized cargo proteins; which constantly undergo endocytosis. Initial evidence suggests a direct binding between BRI1 and AP-2-complex proteins (Rubbo et al., 2013). The current effort is focused on identifying the motifs of cargo protein involved in such interaction. We also mean to identify additional players, if any, of this process. Till date, we have generated/acquired several mutant lines of putative YXXΦ and XLL motifs; the key motifs shown to assist in cargo recognition by AP-2 complex. Whereas the preliminary results seems to rule out any direct involvement of two putative XLL (DERLL and EIELL) and a conserved FSTI motif in affecting BR signaling, it remains to be seen how BRI1 internalization is affected in the mutant XLL transgenic *Arabidopsis* plants. Therefore, additional evidence would be provided by adopting Confocal laser scanning microscopy for BRI1-GFP endocytosis in pBRI1::BRI1-GFP/*bri1-116* and pBRI1::BRI1(M)-GFP/*bri1-116* transgenic lines. Relatively higher sensitivity of pBRI1::BRI1Y898S-mCitrine/*bri1-GABI-Kat* to brassinazole and more resistance of pBRI1::BRI1Y898S-mCitrine/*bri1-Gabi* and pBRI1::BRI1Y956S-mCitrine/*bri1-GABI-Kat* to BL is interesting and indicates towards reduced BR signaling. Moreover, reduced rosette leaf area and partial male sterility of these mutant lines further indicated the reduced BR signaling. Reduced BES1 dephosphorylation further validated that BR signaling is reduced in the BRI1(Y to S) mutants in comparison to their control. Spinning disc laser microscopy revealed that while most of BRI1 at PM remains in steady state and do not undergo active internalization, only a fraction is dynamic in nature. Track length analysis of kymographs on this active fraction showed that time of BRI1 residency is significantly prolonged in the BRI1(Y to S)

mutant lines in comparison to the BRI1mCitrine complemented line. Additionally, more transgenic lines for mutated YXXΦ lines for both Y to S and Y to F substitutions have been generated to substantiate initial observations. The data on kinase activity of BRI1 (Y to S) mutant alleles would help in finding the reason for reduced BR signaling in these transgenic lines. We have also established collaboration with Prof. Steven Huber, Professor of Plant Biology and Crop Sciences, University of Illinois at Urbana-Champaign, USA for performing the kinase assay experiment of normal and mutated BRI1 alleles generated in our laboratory. The data on BRI1 interacting proteins, which remains mostly unchanged even in the absence of functional ARF-GEFs, or in the presence of BL or BFA is encouraging and in order to get comprehensive information on the BRI1 interactome in additional growth conditions can be included for additional IP/MS experiments in future. Altogether, we envisage that the current effort will provide an in-depth understanding of initial steps of BRI1 recognition and its subsequent internalization in plants.

5. Valorisation/Diffusion

To conduct the BRI1-GFP-IP/MS experiments, a short training (from 01/12/2014 to 15/12/ 2014) on the adopted proteomic techniques was done in the lab of Prof. Sacco de Vries, Laboratory of Biochemistry, University of Wageningen, Wageningen, The Netherlands. The same procedure has now been established to conduct similar additional proteomic experiments at PSB/ VIB, University of Ghent.
A part of the work done was presented in the conference, European Network for Plant Endomembrane Research (ENPER) 2015, 17/08/2015-20/08/2015 at the University of Leeds, UK. The FWO-travel grant for the same has also been accorded. In order to get familiar with the Confocal Laser Scanning Microscopy, a conference entitled 'Past, Present and Future Confocal Microscopy' was also attended on 26/3/2015 at Het Pand, Gent.
Additionally, I have contributed to the research article entitled "**AtPep1 induced responses require clathrin mediated endocytosis in *Arabidopsis***" authored by "Ortiz-Morea F A, Kumar R, Luo Y, Dejonghe W, De Oliveira G P, Lu Q, Zhao X, and Russinova E" is in preparation for submission.

6. Skills/Added value transferred to home institution abroad

The BELSPO program provided me an excellent platform to gain postdoctoral research experience and acquire new skills especially in the research fields of molecular cell biology, proteomics and Confocal Laser Scanning Microscopy (CLSM). The experience gained during this program would be transferred to the home institution to introduce the new technologies, especially related to cell biology, CLSM and identifying the interactome *in planta* for candidate proteins. As the use of genomics tools are more prevalent in their research in the home institution, the introduction of the aforementioned tools would help to explore the same research problems in a more holistic manner. The IP/MS procedure, which was employed for identification of BRI1 interacting proteins in *Arabidopsis*, would be tested and trained for its applicability in crop species. Finally, the BELSPO program provided home institution an opportunity to have collaborations with the host institution, in future.

7. Miscellaneous

We sincerely thank Prof. Gregory Vert, Institut des Sciences du Végétal, CNRS, France for sharing their YXXΦ mutant *Arabidopsis* transgenic lines (pBRI1::BRI1Y898S-mCitrine/bri1-*GABI-Kat* and pBRI1::BRI1Y956S-mCitrine/bri1-*GABI-Kat*) with us.

8. References

Bar, M., and Avni, A. (2009). EHD2 inhibits ligand-induced endocytosis and signaling of the leucine-rich repeat receptor-like protein LeEix2.Plant J. 59: 600–611.

Bojar, D et al. Crystal structures of the phosphorylated BRI1 kinase domain and implications for brassinosteroid signal initiation. Plant J. 2014. 78:31–43.

Bonifacino, J.S., and Traub, L.M. (2003). Signals for sorting of transmembrane proteins to endosomes and lysosomes. Annu. Rev. Biochem. 72: 395–447.

Di Rubbo, S et al. The clathrin adaptor complex AP-2 mediates endocytosis of brassinosteroid insensitive1 in Arabidopsis Plant Cell. 2013. 25: 2986–2997.

Fàbregas, N. et al. The BRASSINOSTEROID INSENSITIVE1–LIKE3 Signalosome Complex Regulates *Arabidopsis* Root Development. Plant Cell 2013. 25: 3377–3388.

Geldner, N., and Robatzek, S. (2008). Plant receptors go endosomal: A moving view on signal transduction. Plant Physiol. 147: 1565–1574.

Geldner, N., Hyman, D.L., Wang, X., Schumacher, K., and Chory, J. Endosomal signaling of plant steroid receptor kinase BRI1.Genes Dev. 2007.21: 1598–1602.

Happel, N., Honing, S., Neuhaus, J.M., Paris, N., Robinson, D.G., Holstein, S.E.H. (2004) Arabidopsis μA-adaptin interacts with the tryosine motif of the vacuoler sorting receptor VSR-PS1. Plant J. 37:678-693.

Irani, N. G. et al. Fluorescent castasterone reveals BRI1 signaling from the plasma membrane. Nature Chem. Biol.2012.8: 583-589.

Peyroche, A., Antonny, B., Robineau, S., Acker, J., Cherfils, J., and Jackson, C. L. (1999). Brefeldin A acts to stabilize an abortive ARF-GDP-Sec7 domain protein complex: involvement of specific residues of the Sec7 domain. Mol. Cell 3: 275-285.

Takano, J., Tanaka, M., Toyoda, A., Miwa, K., Kasai, K., Fuji, K., Onouchi, H., Naito, S., and Fujiwara, T. (2010). Polar localization and degradation of Arabidopsis boron transporters through distinct trafficking pathways. Proc. Natl. Acad. Sci. USA 107: 5220–5225.

Traub, L.M (2009). Tickets to ride: selecting cargo for clathrin-regulated internalization. Nat. Rev. Mol. Cell Biol. 10, 583-596.

Wang, Z.-Y. et al. Brassinosteroid Signaling Network and Regulation of Photomorphogenesis. Annu. Rev. Genet. 2012. 46:701–24.